

## Supplementary Equation (related to Extended Data Fig. 7)

### Simple diffusion model

We want to estimate the pH at the location of the putative pH-sensor H207 in TBC1D5, given the flux of protons from NHE6 from the endosomal lumen into the cytosol. In the absence of an experimental structure of the full TBC1D5/Rab7/NHE6 assembly and lack of detailed information for ions, protons, and the NHE6 transport rate, we are only aiming for a highly simplified model. We assume that protons diffuse from the cytosolic exit of NHE6 towards the cytosol (“bulk”), which maintains a constant pH due to the strong buffering of the cytosol and other active processes. We are interested in the proton concentration  $c(\mathbf{r})$  in steady state (no time dependence) that obeys the Laplace equation (diffusion equation without time dependence and no sources or sinks because we consider the proton source to be situated on the boundary of our problem)  $\nabla^2 c = 0$ . We assume Fick’s law for the current  $j = -D\nabla c$  with the diffusion coefficient  $D$ . For simplicity, we will assume that  $D$  is constant and does not depend on position.

### 1D cylindrical diffusion model

In order to solve the diffusion equation analytically we must choose a suitable simple geometry and set boundary conditions. We used our model of the TBC1D5/Rab7/NHE6 dimer complex and traced the shortest path inside the protein from D260 (proton binding site in NHE6) to H207 (proton sensor in TBC1D5) using a custom version of HOLLOW<sup>2</sup>

(<https://github.com/Becksteinlab/hollow>) and networkX<sup>3</sup> for Dijkstra’s algorithm (Figure 1). The putative proton diffusion pathway emerges from the cytosolic access funnel of NHE6 and is confined between Rab7 and TBC1D5, measuring 8.95 nm along the curved path. We approximate this path with a straight cylinder of length  $L = 9.5$  nm with H207 located near  $z = 7.5$  nm along the cylinder axis.

We make additional simplifying assumption (rotational symmetry around the cylinder axis

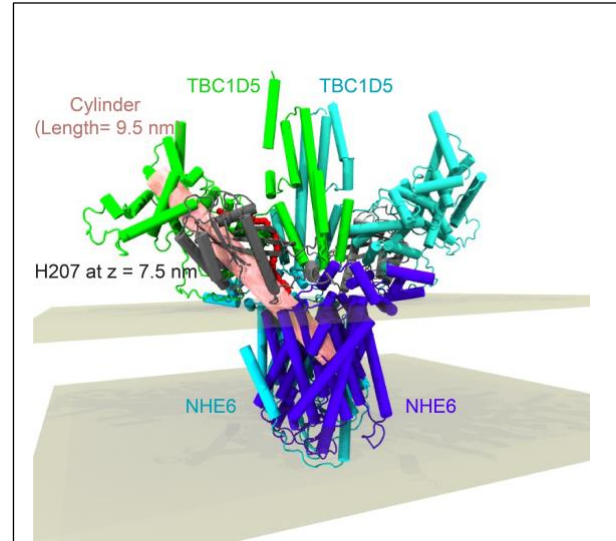


**Figure 1.** Proton diffusion domain (pink semi-transparent cylinder) overlaid on model of the TBC1D5 (green, teal)/Rab7 (gray, light gray)/NHE6 (violet, cyan) dimeric complex. The approximate position of the membrane is indicated by light-gray planes. A possible proton path from the proton-releasing residue D260 in NHE6 to the hypothesized proton sensor H207 in TBC1D5 is shown as red spheres (partially hidden inside the cylinder). The cylinder starts inside NHE6 and ends at the surface of TBC1D5. (Image rendered with VMD<sup>1</sup>)

and no radial dependence) to reduce the 3D diffusion equation to a simple 1D problem  $\frac{\partial^2 c}{\partial z^2} = 0$  for the density  $c(z)$ .

We choose as boundary conditions (1) Bulk proton concentration at  $z = L$ ,  $c(z = L) = c_0$  (with instantaneous absorption) because the buffering capacity of the cytosol is so large that any protons escaping the confinement will immediately be absorbed into the cytosol. (2) Particles enter at  $z = 0$  with a constant current density  $j_0$  (using Fick's law  $j = -D \frac{\partial c}{\partial z}$ )  $\frac{\partial c}{\partial z} \Big|_{z=0} = -\frac{j_0}{D}$ .

The proton current density  $j_0 = k_{H+}/\pi r^2$  is a function of the transporters proton transport rate (turnover)  $k_{H+}$  over the cross-sectional area of the cylinder, where we chose  $r = 0.3$  nm based on the molecular model.

Solving Laplace's equation with the boundary conditions yields the simple linear profile

$$c(z) = c_0 + \frac{j_0}{D}(L - z),$$

which trivially gives the local pH-profile  $pH(z) = -\log_{10} c(z)/1M$  under steady-state condition, i.e., assuming constant turnover of the transporter.

For the bulk we set a concentration  $c_0$  corresponding to pH 7.2<sup>4</sup>.

### Local pH as a function of transporter turnover

In water, protons diffuse fast due to the Grotthuis mechanism with a bulk diffusion coefficient  $D_{H+} = 9.3 \times 10^{-3}$  nm<sup>2</sup>/ps. However, in an environment with many buffer molecules or titratable residues as encountered along the diffusion pathway inside the complex, diffusion can slow down dramatically<sup>5</sup>; in the absence of a detailed simulation we will simply assume that proton diffusion is slowed down by a factor  $0 < \alpha \ll 1$  and work with the *effective proton diffusion coefficient*  $D_{\text{eff}} = \alpha D_{H+}$ . For our initial exploration we assume a conservative value of  $\alpha = 10^{-1}$ .

Sodium-proton antiporters are some of the fastest secondary active transporters with some family members such as NhaA having peak turnover numbers of about 1 ms<sup>-1</sup><sup>6</sup>. We do not know the turnover number of NHE6 so we calculated the local pH profile for a range of reasonable values ranging from 0.25 to 2 ms<sup>-1</sup> in Figure 2. The local pH is reduced

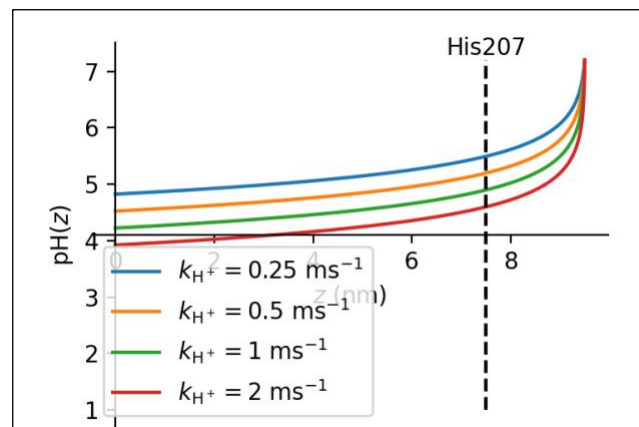


**Figure 2.** Local pH( $z$ ) profile for the cylindrical diffusion model along the path axis ( $z$  in nm), assuming a constant proton production rate  $k_{H+}$ , an effective proton diffusion coefficient of 1/10 of the bulk value, and a bulk pH 7.2. The approximate position of H207 along the diffusion path is indicated.

by 2 to 3 pH units along the path and only raises sharply near the exit to the bulk. Higher turnover rates produce more protons that accumulate near the transporter and only slowly diffuse towards the bulk exit where they are absorbed, leading to lower local pH. The pH near H207 would be predicted to be around 5, likely sufficiently low to change its protonation state. However, our simple model also predicts an unreasonably acidic local pH between 4 and 5 at the transporter, primarily due to our assumption of a constant transporter turnover rate.

There are two reasons why a cation/proton antiporter (CPA) such as NHE6 may not function with such a low pH. Transport must be thermodynamically favored and typical CPAs only transport in a relatively narrow pH activity window<sup>7</sup>.

### Thermodynamics of 1:1 antiport

The commonly ascribed physiological role of NHE6 in endosomes is that of a leak pathway for protons that prevents over-acidification of the endosome and helps maintain the endosome pH. Therefore, we are interested in the transport of protons from the inside of the endosome to the cytosol. We will denote transport in this direction with a negative sign and transport from the cytosol into the endosome with a positive sign. Thus, moving one proton into the cytosol counts as  $-1$  and one cation from the cytosol into the endosome as  $+1$ .

Assuming perfect coupling between proton  $H^+$  and driving cation  $X^+$  transport in a 1:1 antiport stoichiometry, the free energy dissipation per transport cycle (where the  $\Delta\mu$  are the electrochemical potential differences between inside (endosomal lumen) and outside (cytosol),  $k$  is Boltzmann's constant, and  $T$  is the temperature) is:

$$\begin{aligned}\Delta G &= \Delta\mu_{X^+} - \Delta\mu_{H^+} < 0 \\ kT\ln(c_{X^+}^{in}/c_{X^+}^{out}) - kT\ln(c_{H^+}^{in}/c_{H^+}^{out}) &< 0 \\ c_{X^+}^{in}/c_{X^+}^{out} &< c_{H^+}^{in}/c_{H^+}^{out}\end{aligned}$$

and because of the second law of thermodynamics, this dissipation must be negative (with our convention of signs<sup>8</sup>) — i.e., the free energy available from the driving cation must be more negative than the energetic cost of the proton transport.

Thus, the proton concentration on the outside (cytosolic side) must obey

$$c_{H^+}^{out} < c_{H^+}^{in} (c_{X^+}^{out}/c_{X^+}^{in})$$

so that any vectorial transport of protons from the endosome to the cytosol is possible. (Note that this relation does not determine the actual rate of transport,  $k_{H^+}$ , which requires a detailed kinetic analysis and requires more information about the individual steps of the transport cycle, see e.g.,<sup>9</sup>.) Equivalently, the local pH must satisfy

$$pH^{out} > pH^{in} - \log_{10}(c_{X^+}^{out}/c_{X^+}^{in}).$$

## Physiological concentrations and driving forces

For the late endosome and the cytosol, pH and ion concentrations are:

Ion	Inside (late endosome)	Outside (cytosol)	Reference
$\text{Na}^+$	20-140 mM	~12 mM	<sup>10</sup>
$\text{K}^+$	2-50 mM	~150 mM	<sup>10</sup>
$\text{H}^+$	pH 5.5-5.8	pH 7.2	<sup>11</sup>

For our model we will assume extreme values (in bold face) to get a better sense of the range of behavior.

The free energy to move a proton from the outside to the inside would be  $3.9 \text{ } kT$ , which is positive and unfavorable. Moving the proton from the inside to the outside is favorable with the negative of this value,  $-3.9 \text{ } kT$ . Thus, protons would spontaneously move from the endosome to the cytosol. At first glance, no driving ion is needed because no thermodynamic driving force is needed for the energetically downhill spontaneous proton movement, although any additional driving force would accelerate proton transport.

The gradient for sodium ions is *also* directed from endosome to the cytosol, in the same direction as the proton gradient. Because of NHE6's antiporting mechanism, the sodium driving force

$$\Delta\mu_{\text{Na}^+} = kT \ln(c_{\text{Na}^+}^{\text{in}}/c_{\text{Na}^+}^{\text{out}})$$

will effectively *hinder* proton movement. Its magnitude is  $2.5 \text{ } kT$ . The proton driving force is stronger and thus the proton gradient can **drive accumulation of sodium into the endosome** and NHE6 would function as a proton-driven sodium transporter. (Below we will compute maximum cytosolic pH if only  $\text{H}^+/\text{Na}^+$  transport were possible).

NHE6 is known to also transport **potassium ions**<sup>12</sup> and the  $\text{K}^+$  gradient is directed from the cytosolic side towards the endosome and can thus drive proton efflux. Its magnitude is  $-4.3 \text{ } kT$ . This is a strong thermodynamic driving force that can additionally **drive proton export into the cytosol**.

The proton **and** potassium gradients **favor transport cycles that export protons**. Only sodium transport is energetically uphill.

## Transport of a single cation

Under the assumption that only one cation drives the transport, the cytosolic pH near the transporter exit must obey  $\text{pH}^{\text{out}} > \text{pH}^{\text{in}} + \log_{10}(c_{X^+}^{\text{in}}/c_{X^+}^{\text{out}})$  as derived above. Both potassium and protons have energetically downhill gradients but the potassium gradient is stronger. Therefore, **potassium** could drive proton export and *generate*  $\text{pH}^{\text{out}} > 3.6$ , i.e., **accumulate**

**protons on the outside below the endosomal pH.** If NHE6 were to solely function as a potassium/proton exchanger then the local pH at the cytosolic exit could not be lower than pH 3.6. However, we already remarked that this is a physiologically unrealistically low pH.

Alternatively, **sodium** can be driven by the proton gradient, which results in  $\text{pH}^{\text{out}} > 6.6$ . In this way, NHE6 exports protons from the endosome to the cytosol and accumulates sodium in the endosome. If NHE6 were to solely function as a sodium/proton exchanger then the local pH at the cytosolic exit could not be lower than pH 6.6.

However, in principle **both** ions may be transported, just not in the same transport cycle.

### **Na<sup>+</sup> and K<sup>+</sup> with proton transport**

NHE6 can go through a transport cycle with 1:1 proton:sodium stoichiometry or through an alternative one with 1:1 proton:potassium stoichiometry. On average, we can express the probability to go through each of these cycles with the effective stoichiometries  $m_{\text{Na}^+}$  and  $m_{\text{K}^+}$  with  $m_{\text{Na}^+} + m_{\text{K}^+} = 1$ . The effective transport stoichiometry is  $m_{\text{Na}^+}:m_{\text{K}^+}:1$ , which means that on average for each proton,  $m_{\text{Na}^+}$  sodium ions and  $m_{\text{K}^+}$  potassium ions are transported. Then the effective free energy generation per cycle is

$$\Delta G = m_{\text{Na}^+} \Delta \mu_{\text{Na}^+} + m_{\text{K}^+} \Delta \mu_{\text{K}^+} - \Delta \mu_{\text{H}^+} < 0$$

$$m_{\text{Na}^+} kT \ln(c_{\text{Na}^+}^{\text{in}}/c_{\text{Na}^+}^{\text{out}}) + m_{\text{K}^+} kT \ln(c_{\text{K}^+}^{\text{in}}/c_{\text{K}^+}^{\text{out}}) - kT \ln(c_{\text{H}^+}^{\text{in}}/c_{\text{H}^+}^{\text{out}}) < 0$$

and then the limiting external pH would be

$$pH^{\text{out}} > pH^{\text{in}} + (\ln 10)^{-1} \left( m_{\text{Na}^+} \ln(c_{\text{Na}^+}^{\text{in}}/c_{\text{Na}^+}^{\text{out}}) + m_{\text{K}^+} \ln(c_{\text{K}^+}^{\text{in}}/c_{\text{K}^+}^{\text{out}}) \right)$$

The effective stoichiometries depend on the microscopic rates as well as external concentrations. In the following we will use a simple model that only considers concentrations.

With a competitive binding model where we can have 1 sodium *or* 1 potassium bound or neither (empty), the probability for binding either sodium or potassium is

$$m_{\text{Na}^+} \approx c_{\text{Na}^+} K_{d,\text{Na}^+}^{-1} / (c_{\text{Na}^+} K_{d,\text{Na}^+}^{-1} + c_{\text{K}^+} K_{d,\text{K}^+}^{-1} + 1)$$

$$m_{\text{K}^+} \approx c_{\text{K}^+} K_{d,\text{K}^+}^{-1} / (c_{\text{Na}^+} K_{d,\text{Na}^+}^{-1} + c_{\text{K}^+} K_{d,\text{K}^+}^{-1} + 1)$$

where the binding constants for sodium and potassium are being used; if the ions bound strongly  $cK_d^{-1} \gg 1$  then we could immediately omit the empty state contribution (+1 term in the denominator). Typical values for ion binding in the NapA sodium/proton antiporter are  $K_d \approx 1 \text{ mM}^{13}$  and we will assume that NHE6 similarly only binds cations weakly. However, with the given concentrations, the denominator always contains at least one term that is at least 100 times larger than 1 and hence the +1 term can be neglected.

To further simplify, assume that sodium and potassium bind equally strongly,  $K_{d,\text{Na}^+} \approx K_{d,\text{K}^+} \equiv K_d$  and hence

$$m_{\text{Na}^+} \approx c_{\text{Na}^+}/(c_{\text{Na}^+} + c_{\text{K}^+})$$

$$m_{\text{K}^+} \approx c_{\text{K}^+}/(c_{\text{Na}^+} + c_{\text{K}^+})$$

Given that the cytosol has the larger reservoir of ions than the endosome, we make the simplifying assumption that the *stoichiometric ratio is only determined by the cytosolic (outside) concentrations*; realistically, all other forward and backwards rates and concentrations may also affect the probabilities to follow different transport cycles but we ignore them here. The concentrations of sodium and potassium differ by at least one order of magnitude on the outside ( $\sim 12.5$ ) and hence the stoichiometric ratio skews strongly towards  $\text{K}^+$  with  $m_{\text{K}^+} = 0.926$  and  $m_{\text{Na}^+} = 0.074$ .

Taken together, the effective limiting outside pH is

$$\text{pH}^{\text{out}} > \frac{m_{\text{K}} \ln \left( \frac{c_{\text{K}}^{\text{in}}}{c_{\text{K}}^{\text{out}}} \right) + m_{\text{Na}} \ln \left( \frac{c_{\text{Na}}^{\text{in}}}{c_{\text{Na}}^{\text{out}}} \right)}{\ln(10)}$$

and with physiological values we obtain  $\text{pH}^{\text{out}} > 3.84$ . This limiting pH is only marginally larger than the one for only potassium (3.62, see above) because many more transport cycles involve potassium than sodium. It is also lower than the endosome internal pH because the favorable potassium gradient is used to additionally pump protons in the opposite direction into the cytosol. Physiologically, this is an extremely low pH that would not be realized in the cell.

### No thermodynamic limiting condition but kinetic limitation

If the above assumptions hold then NHE6 will only transport protons from the endosome to the cytosol while the outside pH is greater or equal to 3.84 (although we do not really know the transport rate).

This pH is unphysiologically acidic. However, **the above calculation indicates that under the given conditions, there is no real thermodynamic limit to the pH at the transporter exit.**

Instead, these calculations suggest that **NHE6 is kinetically limited** and its turnover rate changes as to limit the local cytosolic pH.

Sodium/proton antiporter typically display a pH range in which they are active (e.g. pH 6.5 - 9.0). We do not know the activity range of NHE6. We therefore make the assumption that it does not transport below cytosolic pH 5.5 (i.e., if the cytosolic pH would equal the pH of the lumen).

In the following we will also make the simplifying assumption that the transport rate does not depend on the external concentrations of ions/protons. (This is almost certainly not true, see for an example the simplified sodium/proton antiporter in Fig 7a in Kenney & Beckstein 2023<sup>14</sup>

where the turnover number is shown to depend on the sodium concentration.) We can then calculate an effective limiting transport rate  $j_{0,\max}$  by solving the analytical solution for  $c(z = 0)$  at the limiting concentration  $c_{\max} = 10^{-\text{pH}^{\text{out}}}$

$$c(z = 0) = c_0 + \frac{j_0(L - z)}{D} < c_{\max}$$

to find the maximum current  $j_{0,\max} < \frac{D(-c_0 + c_{\max})}{L}$  (or proton transport rate) and the concentration profile as a function of the maximum concentration

$$c(z) = c_0 + \frac{(L - z)(-c_0 + c_{\max})}{L}.$$

(Of course, we could have just solved the Laplace equation directly with the boundary conditions  $c(z = 0) = c_{\max}$  and  $c(z = L) = c_0$  and arrived at the same result.) Note that the concentration gradient does not depend on the (effective) proton diffusion coefficient because if the transporter is fast enough to generate a local pH at the thermodynamic limit, then it does not matter how fast protons diffuse away. Under these conditions the effective proton transport rate would be  $k_{H^+, \max} = 0.052 \text{ ms}^{-1}$ , i.e., a very small effective turnover number may be sufficient (which is *much* lower than the known high turnover number of  $1 \text{ ms}^{-1}$  for other sodium/proton antiporters).

With this effective proton transport rate (or equivalently, a minimum local pH 5.5 at the cytosolic exit of NHE6), the concentration profile has the shape shown in Figure 3. The local pH( $z$ ) rises monotonically from 5.5 at the cytosolic release site of NHE6 to the bulk value of 7.2 at  $z=9.5 \text{ nm}$ . Near the location of H207 at  $z=7.5 \text{ nm}$  the local pH is 6.15 and remains substantially lower than bulk. In solution, histidine has a pKa of  $\sim 6.0$ . In TBC1D5, H207 is completely buried and PROPKA 3.1<sup>15</sup> predicts an elevated pKa of 6.39. Thus, a local pH of 6.15 would shift H207's protonation state towards protonation (and positively charged) compared to its mostly deprotonated (neutral) state near bulk pH 7.2.

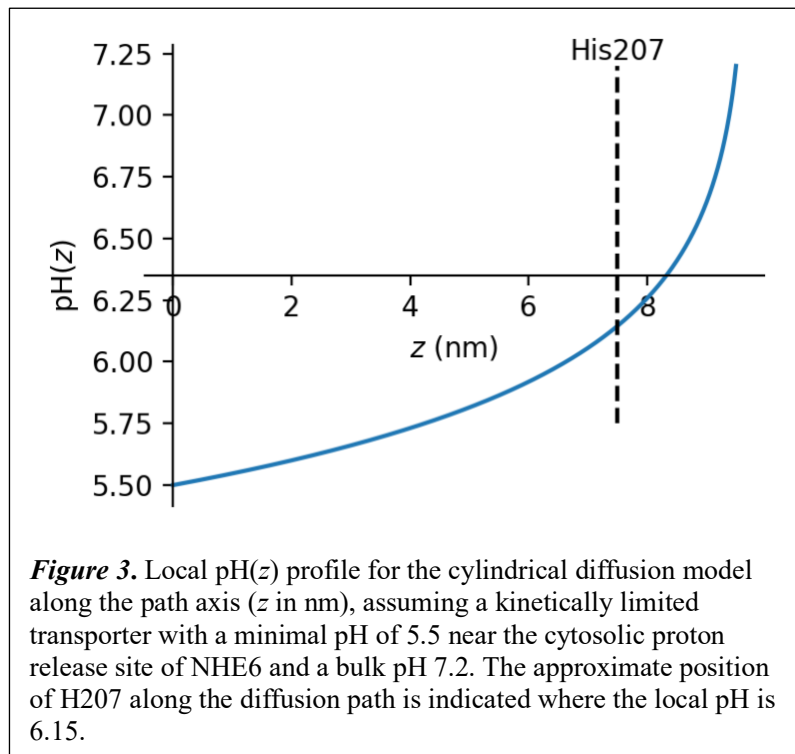


**Figure 3.** Local pH( $z$ ) profile for the cylindrical diffusion model along the path axis ( $z$  in nm), assuming a kinetically limited transporter with a minimal pH of 5.5 near the cytosolic proton release site of NHE6 and a bulk pH 7.2. The approximate position of H207 along the diffusion path is indicated where the local pH is 6.15.

## Summary – 1D diffusion model

1. Proton efflux from the endosome to the cytosol is thermodynamically favorable.
2. If the proton efflux is mediated by the NHE6 cation/proton exchanger (antiporter) then export of one proton would be coupled to an import of one cation.
3. The proton gradient can drive energetically uphill import of sodium into the endosome. The potassium gradient (directed towards the endosome) can drive proton export. A simple model suggests that potassium/proton exchange is the primary transport cycle.
4. If NHE6 were to run at full turnover *and* proton diffusion away from the cytosolic exit is slowed down (due to localized titratable groups) then a very strong local pH gradient could be maintained. However, CPAs typically only operate in a narrow pH activity window, which may limit the achievable pH gradient.
5. At 7.5 nm away from the transporter exit, the pH near His207 may be sufficiently different from the bulk to lead to a change in His protonation state.

## (Poor) Hemispherical (3D) diffusion model

We also investigated a model for which we assume that protons diffuse isotropically into the hemisphere above the proton binding site near D260 (NHE6) with a reduced diffusion coefficient. At the outer sphere boundary at  $R=9$  nm they are absorbed into bulk at pH 7.2. Protons are emitted from the center of the transporter and for mathematical convenience we chose a hemispherical emitter of radius  $r_H = 0.3$  nm (Figure 4). H207 would be located at a radial distance of 7.5 nm.

This model leads to a different form of the concentration profile

$$c(r) = c_0 + \frac{Rr_H(c_{max}-c_0)(r^{-1}-R^{-1})}{R-r_H}$$

and with a limiting pH of 5.5 at NHE6 to a pH of 7.07 near H207, which seems insufficient to elicit a measurable response.

The hemispherical model assumes that protons diffuse freely and isotropically in space as if the protein (and the membrane) were highly porous to protons. Inspection of our structural model indicates that this is an incorrect assumption and that the 1D cylindrical model much better captures the well-defined solvent accessible pathways that are formed primarily at the interfaces of the subunits.

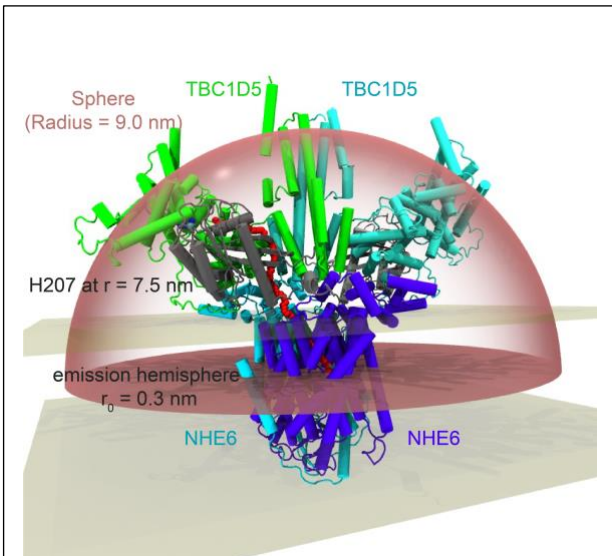


**Figure 4.** Hemispherical (3D) diffusion model. Proton diffusion domain (pink semi-transparent hemisphere) overlaid on model of the TBC1D5 (green, teal)/Rab7 (gray, light gray)/NHE6 (violet, cyan) dimeric complex. The approximate position of the membrane is indicated by light-gray planes. A possible proton path from the proton-releasing residue D260 in NHE6 to the hypothesized proton sensor H207 in TBC1D5 is shown as red. (Image rendered with VMD <sup>1</sup>)

## References

- 1 Humphrey, W., Dalke, A. & Schulten, K. VMD: visual molecular dynamics. *J Mol Graph* **14**, 33-38, 27-38 (1996). [https://doi.org/10.1016/0263-7855\(96\)00018-5](https://doi.org/10.1016/0263-7855(96)00018-5)
- 2 Ho, B. K. & Gruswitz, F. HOLLOW: generating accurate representations of channel and interior surfaces in molecular structures. *BMC Struct Biol* **8**, 49 (2008). <https://doi.org/10.1186/1472-6807-8-49>
- 3 Hagberg, A. A., Schult, D.A, Swart, P.J. Exploring network structure, dynamics, and function using networkX. *Proc. SciPy2008* (2008).
- 4 Theillet, F. X. *et al.* Physicochemical properties of cells and their effects on intrinsically disordered proteins (IDPs). *Chem Rev* **114**, 6661-6714 (2014). <https://doi.org/10.1021/cr400695p>
- 5 Junge, W. & McLaughlin, S. The role of fixed and mobile buffers in the kinetics of proton movement. *Biochim Biophys Acta* **890**, 1-5 (1987). [https://doi.org/10.1016/0005-2728\(87\)90061-2](https://doi.org/10.1016/0005-2728(87)90061-2)
- 6 Taglicht, D., Padan, E. & Schuldiner, S. Overproduction and purification of a functional Na<sup>+</sup>/H<sup>+</sup> antiporter coded by nhaA (ant) from Escherichia coli. *J Biol Chem* **266**, 11289-11294 (1991).
- 7 Calinescu, O. & Fendler, K. A universal mechanism for transport and regulation of CPA sodium proton exchangers. *Biol Chem* **396**, 1091-1096 (2015). <https://doi.org/10.1515/hsz-2014-0278>
- 8 Beckstein, O. & Naughton, F. General principles of secondary active transporter function. *Biophys Rev (Melville)* **3**, 011307 (2022). <https://doi.org/10.1063/5.0047967>
- 9 Awtry, N. C. & Beckstein, O. Kinetic Diagram Analysis: A Python Library for Calculating Steady-State Observables of Biochemical Systems Analytically. *J Chem Theory Comput* **20**, 7646-7666 (2024). <https://doi.org/10.1021/acs.jctc.4c00688>
- 10 Xu, H. & Ren, D. Lysosomal physiology. *Annu Rev Physiol* **77**, 57-80 (2015). <https://doi.org/10.1146/annurev-physiol-021014-071649>
- 11 Ma, L., Ouyang, Q., Werthmann, G. C., Thompson, H. M. & Morrow, E. M. Live-cell Microscopy and Fluorescence-based Measurement of Luminal pH in Intracellular Organelles. *Front Cell Dev Biol* **5**, 71 (2017). <https://doi.org/10.3389/fcell.2017.00071>
- 12 Gao, A. Y. L., Lourdin-De Filippis, E., Orlowski, J. & McKinney, R. A. Roles of Endomembrane Alkali Cation/Proton Exchangers in Synaptic Function and Neurodevelopmental Disorders. *Front Physiol* **13**, 892196 (2022). <https://doi.org/10.3389/fphys.2022.892196>
- 13 Coincon, M. *et al.* Crystal structures reveal the molecular basis of ion translocation in sodium/proton antiporters. *Nat Struct Mol Biol* **23**, 248-255 (2016). <https://doi.org/10.1038/nsmb.3164>
- 14 Kenney, I. M. & Beckstein, O. Thermodynamically consistent determination of free energies and rates in kinetic cycle models. *Biophys Rep (N Y)* **3**, 100120 (2023). <https://doi.org/10.1016/j.bpr.2023.100120>
- 15 Sondergaard, C. R., Olsson, M. H., Rostkowski, M. & Jensen, J. H. Improved Treatment of Ligands and Coupling Effects in Empirical Calculation and Rationalization of pKa Values. *J Chem Theory Comput* **7**, 2284-2295 (2011). <https://doi.org/10.1021/ct200133y>